Electronic Supplementary Material (ESI) for Nanoscale.

Supporting Information

Hierarchical Dual-Porosity Nanoscale Nickel Cermet Electrode with High Performance and Stability

Jingyi Chen,[a] Xin Wang,[a] Paul Boldrin,[b] Nigel P. Brandon,[c]* Alan Atkinson[a]*

a. Department of Materials, Imperial College, London, SW7 2AZ, United Kingdom

b. Department of Earth Science and Engineering, Imperial College, London, SW7 2AZ, United Kingdom

c. Faculty of Engineering, Imperial College, London, SW7 2AZ, United Kingdom

alan.atkinson@imperial.ac.uk

n.brandon@imperial.ac.uk

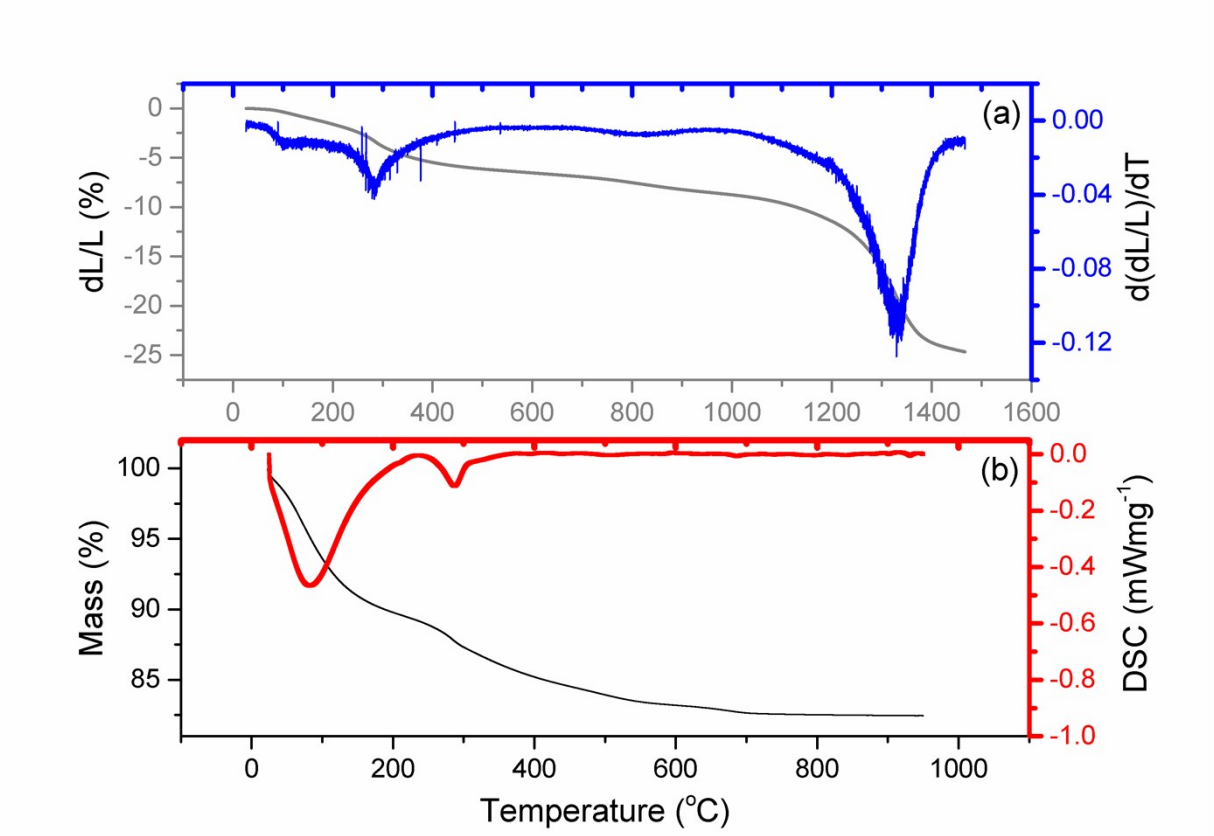

Figure S1 Thermal properties of the NiO-YSZ powder. (a) dilatometry of the freeze-dried NiO-YSZ green pellet: linear shrinkage and shrinkage rate vs. temperature (b) DSC and TGA of the freeze-dried NiO-YSZ powder from room temperature to 950 °C

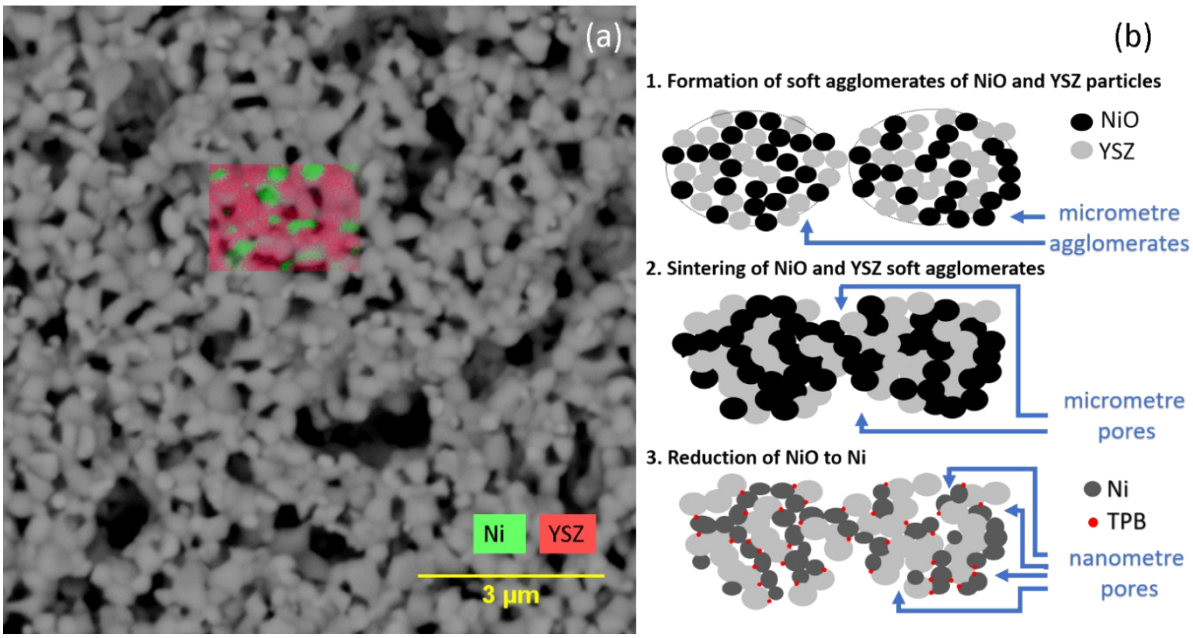

Figure S2 The dual porosity microstructure (a) EDX mapping on the top surface of the Ni-YSZ electrode combined with back-scattered electron image. The green region represents where Ni is detected and red region, Zr. (b) schematic showing the evolution of the microstructure in the fabrication route after 1) calcination and ball milling 2) sintering and 3) reduction.

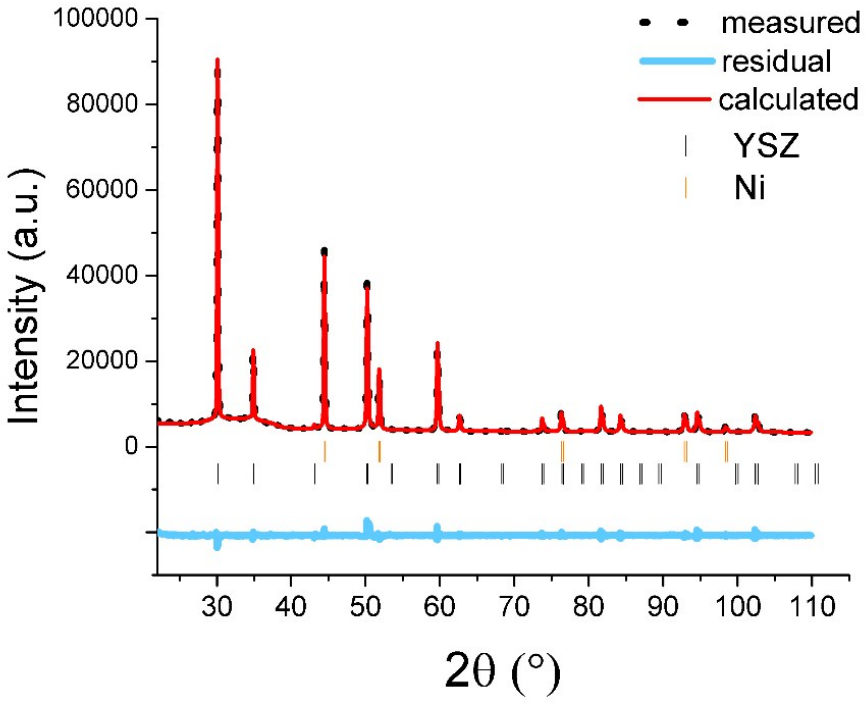

Figure S3 XRD of the Ni-YSZ electrode cast on a YSZ substrate and the Rietveld refinement on the XRD pattern

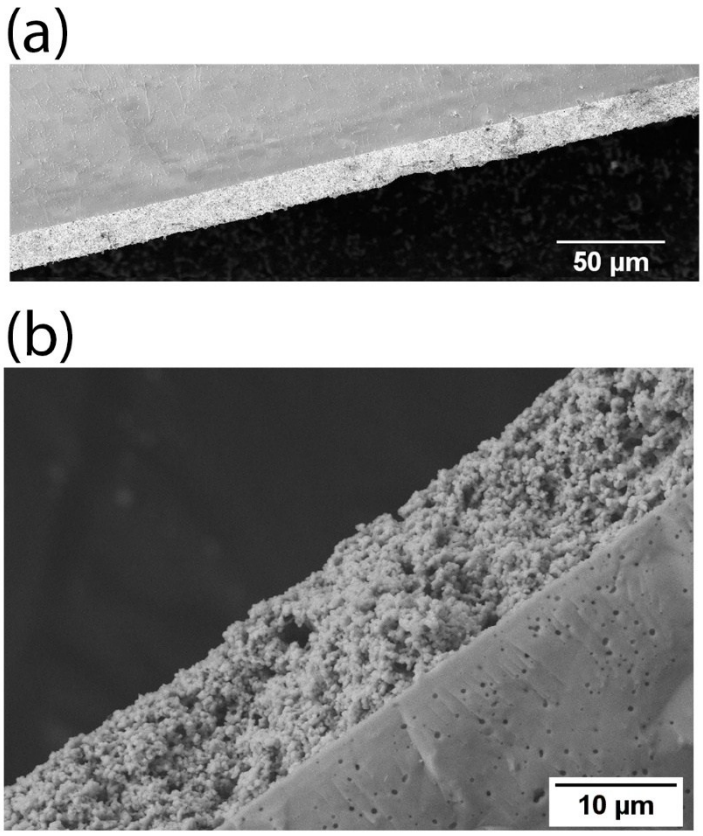

Figure S4 Cross-sectional view of the Ni-YSZ electrode on the YSZ electrolyte for the electrode E1 reduced and aged for 1 h (a) and the E100 aged for 100 h (b).

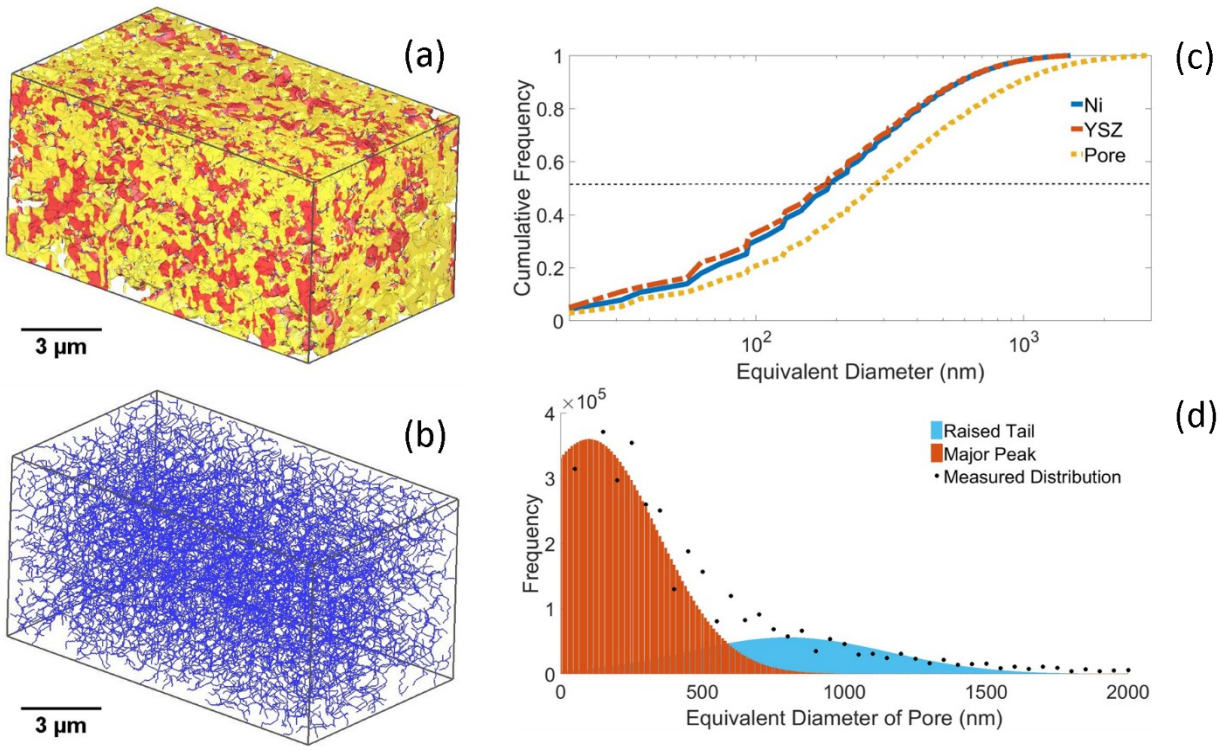

Figure S5 3D reconstruction from FIB-SEM image sequence. (a) 3D reconstructed volume of the Ni-YSZ electrode. The red region represents Ni and the yellow region YSZ. Porosity is represented as transparent hollow space. (b) Percolated TPB network inside the 3D reconstructed volume. (c) Cumulative frequency curves for the equivalent diameter for the three phases, Ni, YSZ and pores measured from the 3D reconstructed volume. The average particle sizes are determined from the 50th percentile (indicated by the dotted line). (d) Frequency distribution of the pore size, showing a major peak at approximately 200 nm and a raised tail at 1000 nm.

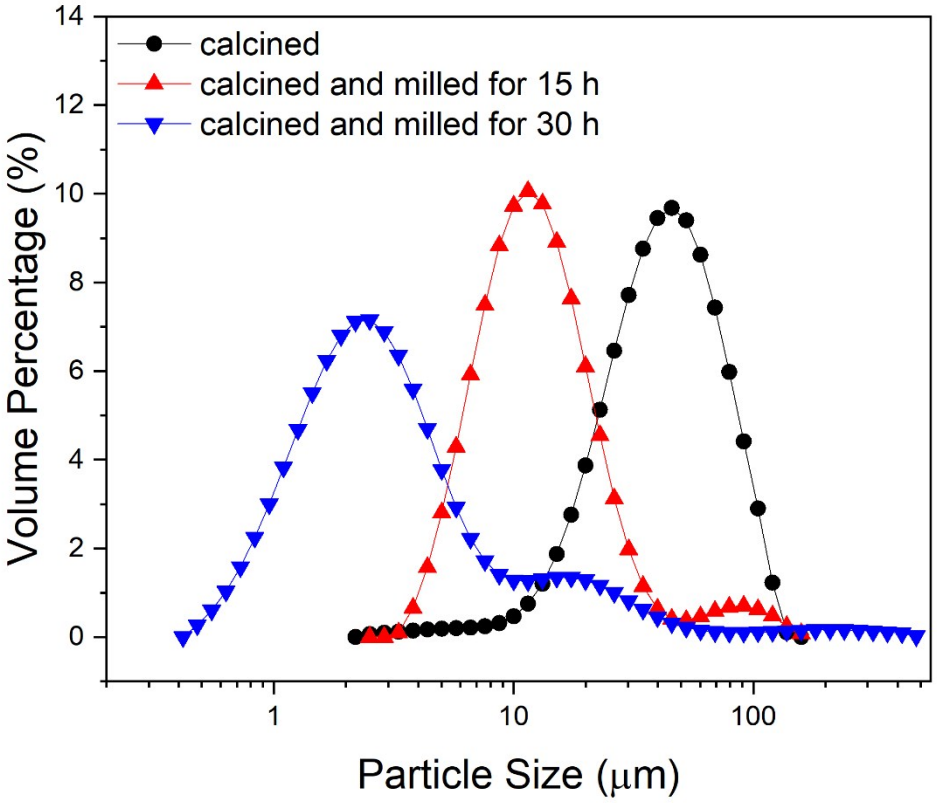

Figure S6 particle size distribution measured by laser light scattering for the freeze-dried powder after 1)calcination 2)calcination and milling for 15 h at 300 rpm and 3)calcination and milling for 30 h at 300 rpm. The calcination was done in air at 700 °C for 30 min.

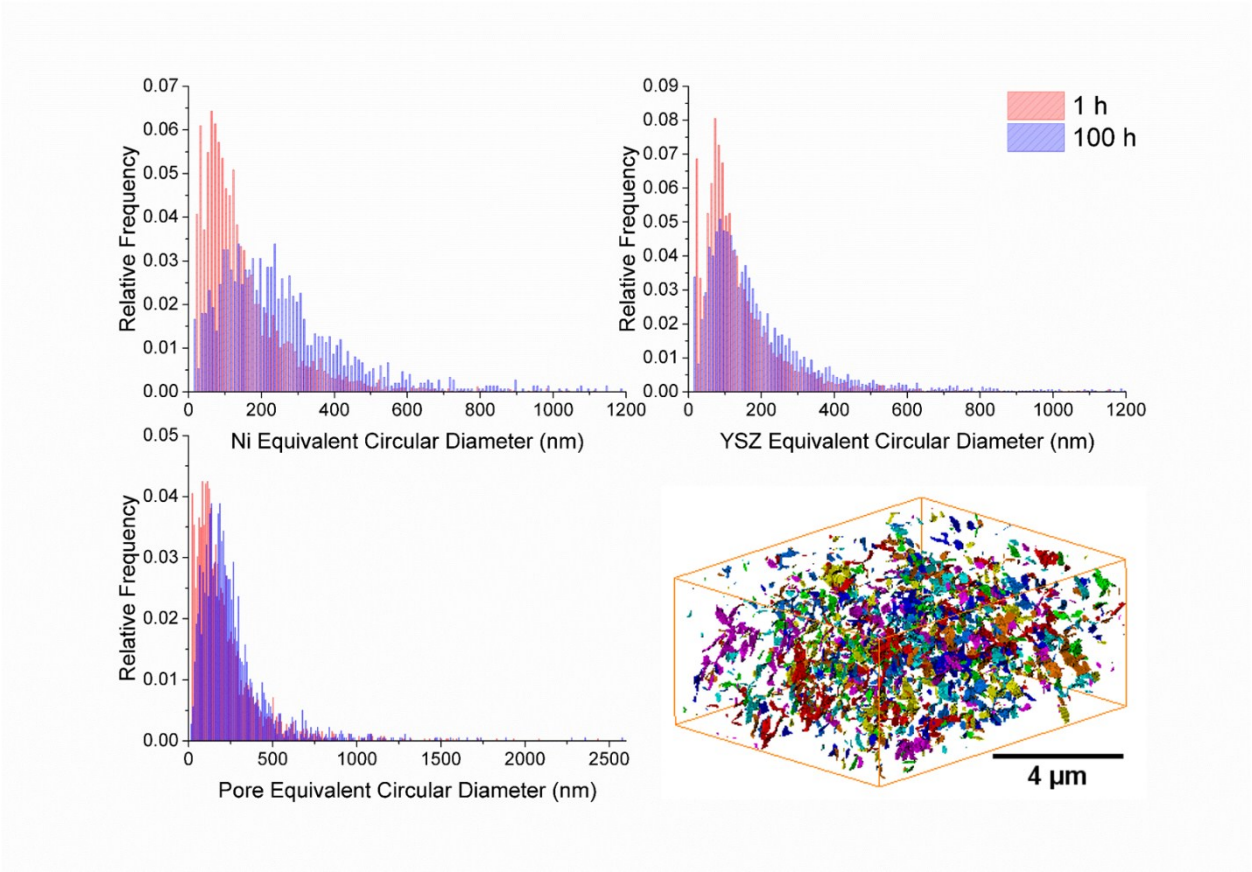

Figure S7 the distribution of the neck diameter for the three networks, Ni, YSZ and pore in E1 after 1h aging and E100 after 100 h aging. The necks are the contact areas shared by neighbouring particles. The 3D volume visualises the necks, indicated by different colours, in the Ni network in E100.

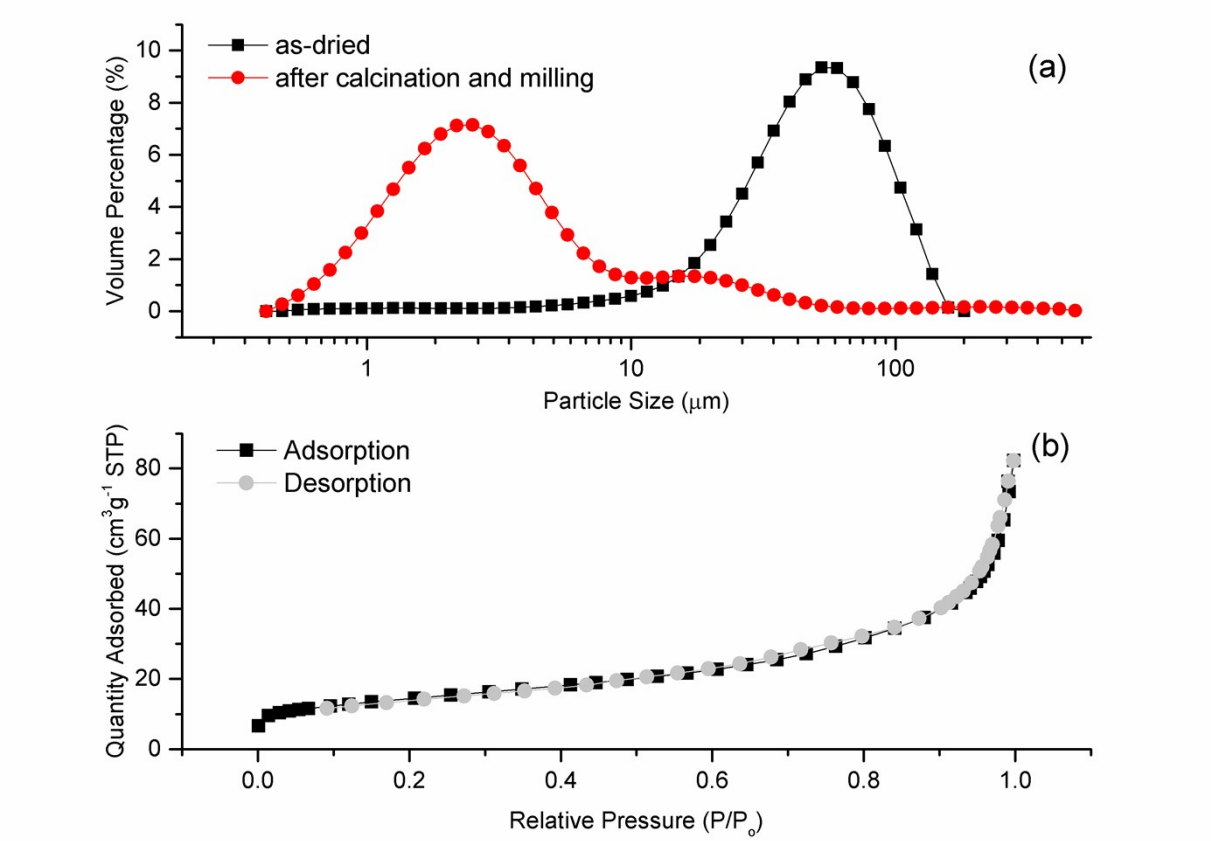

Figure S8 NiO-YSZ powder size distribution and surface area measurements. (a)The particle size distribution measured by laser scattering as-dried and after calcination and milling. (b) Adsorption and desorption isotherm of N_2 at 77 K of the NiO-YSZ nano-composite powder after calcination and ball milling.

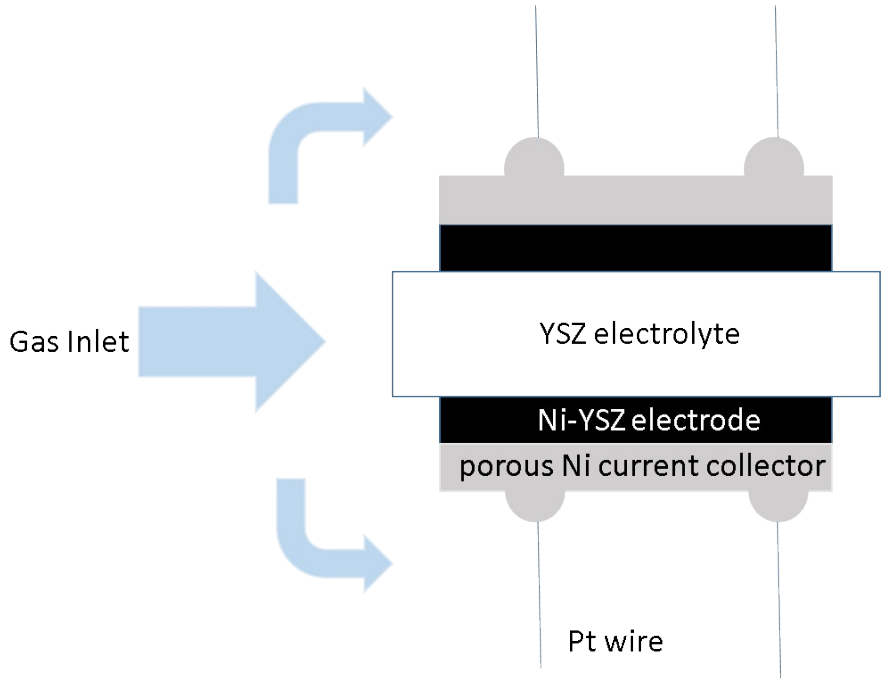

Figure S9 Schematic diagram of the impedance measurement arrangement

Table S1 Values from Complex Nonlinear Least Square (CNLS) fitting on the impedance spectrum in Figure 3d with the equivalent circuit of two R-CPEs and one Gerischer.

	High Frequency	Medium Frequency	Low Frequency
Resistance (R)	0.10	0.48	0.34
Capacitance (F)	2×10^{-4}	2×10^{-3}	5×10^{-2}
CPE n exponential	1	N.A.	0.5

Table S2 The information of the FIB-SEM 3D reconstruction of the two electrode E1 and E100. In humidified 5% H_2-N_2 at 800 °C. E1 underwent 1 h annealing and E100 underwent 100 h annealing.

	E1	**E100**
Dimension of volume imaged x-y-z (μm)	6.8 × 3.7 × 6.0	8.3 × 4.5 × 10.3
Pixel size of volume analysed x-y-z (nm)	16.4 × 16.4 × 20.0	13.8 × 13.8 × 20.0
Volume fraction Pore-Ni-YSZ (%)	39.3-27.3-33.4	34.3-27.2-38.5